

A new method for high energy beam energy measurement with microwave-beam Compton backscattering

Meiyu Si, Shanhong Chen, Pengcheng Wang, Zhe Duan, Manqi Ruan, Yiwei Wang, Guangyi Tang, and Ouzheng Xiao
Institute of High Energy Physics, Chinese Academy of Sciences, Beijing 100049, China

Yongsheng Huang*
*School of Science, Sun Yat-Sen University, Shenzhen 528406, China and
Institute of High Energy Physics, Chinese Academy of Sciences, Beijing 100049, China*

Xiaofei Lan
Physics and Space Science College, China West Normal University, Nanchong 637009, China

Yuan Chen
National Synchrotron Radiation Laboratory, University of Science and Technology of China, Hefei 230029, China

Xinchou Lou and Jianyong Zhang
*Institute of High Energy Physics, Chinese Academy of Sciences, Beijing 100049, China and
State Key Laboratory of Particle Detection and Electronics,
Institute of High Energy Physics, CAS, Beijing 100049, China*

The energy measurement uncertainty of circular electron positron collider (CEPC) beam must be less than 10MeV to accurately measure the mass of the Higgs/W/Z boson. A new microwave-beam Compton backscattering method is proposed to measure the beam energy by detecting the maximum energy of scattered photons. The uncertainty of the beam energy measurement is 6MeV. The detection accuracy of the maximum energy of scattered photons need to reach 10^{-4} . The high-precision gamma detectors can only be a high-purity germanium (HPGe) detector. It is a semiconductor detector, the effective detection range of the gamma energy is 100keV-10MeV. The maximum energy of the scattered photons is chosen to be the higher the better to reduce the influence of the synchrotron radiation background. Therefore, the maximum energy of the scattered photons is selected to be 9MeV. Therefore, the initial photons should be microwave photons to collide with the electrons with the energy of 120GeV on CEPC. The cylindrical resonant cavity with TM_{010} mode is selected to transmit microwaves. After Compton backscattering, the scattered photons emit from the vacuum tube of the synchrotron radiation and the energy is detected by the HPGe detector. The structure of shielding materials with polyethylene and lead is designed to minimize the background noise, such as the synchrotron radiation and the classical radiation from the electron beam in the cavity. The hole radius in the side wall of the cavity is about 1.5mm to allow the electron beam to pass through. The computer simulation technology (CST) software shows that the influence of the hole radius on the cavity field is negligible, and the influence of the hole radius on the resonance frequency can be corrected easily.

I. INTRODUCTION

In 2012, the Higgs boson was discovered by ATLAS and CMS at CERN's large hadron collider (LHC)[1, 2]. In order to study the Higgs boson, a new generation of circular electron positron collider (CEPC) was proposed, which using the electron positron collision to generate 240GeV of center of mass energy[3]. As a Higgs factory, it can further measure the properties of Higgs boson and accurately test the predictions of the standard model. It can also work in W (80GeV) and Z(45.5GeV) mode[3], looking for clues of the new physics beyond the standard model.

The precise measurement of CEPC beam energy is the basic experimental basis for the precise measurement of Higgs/W/Z boson mass. Therefore, a system needs to be designed to accurately measure the beam energy. There are two effective methods to measure the energy of high energy electron beam. (1) The resonant depolarization (RDP) technique. The large electron positron (LEP) collider uses the resonance depolarization method to measure the 45.5GeV beam energy, and the relative uncertainty is 2×10^{-5} [4]. However, the RDP method is difficult to use on CEPC with the beam energy of 120GeV because it is too low to obtain the expected equilibrium degree of

* huangysh59@mail.sysu.edu.cn

beam polarization with state of the art polarimeters. (2) The laser Compton backscattering method. Considering the head-to-head collision between the laser and the electron beam, the beam energy is measured by measuring the positions of scattered electrons, scattered photons, and un-scattered beams downstream of the magnetic system. In the Higgs mode of CEPC, the uncertainty of the beam energy measurement is 2MeV[5]. The precision can meet the physical requirements, but this method has high requirements for the system design and detectors in the future. It needs to design a separate extraction beamline and to use high spatial-resolution and large-area detectors to detect the two-dimensional spatial position of scattered electrons, scattered photons and un-scattered beams respectively.

For Beijing electron positron collider (BEPC II), the electron beam collides with the CO_2 laser to produce scattered photons with the maximum energy of 6MeV. By accurately measuring the maximum energy of the scattered photons, the beam energy measurement uncertainty reached 1.2×10^{-5} [6]. If the beam energy of 120 GeV on CEPC can be measured by measuring the maximum energy of scattered photons, and the measurement accuracy of beam energy can reach 10^{-5} . The detection accuracy of the maximum energy of scattered photons needs to reach 10^{-4} . The high-precision calorimeter of photons is high-purity germanium (HPGe) detectors. But the accurate calibration could be performed in the photon energy within 1 to 10MeV by using of the γ -active radionuclides. In order to reduce the maximum energy of scattered photons to this range, there are two methods. (1) Reducing the collision angle. To generate the scattered photon energy within 10MeV, the collision angle between the laser and the beam is required to be about 0.04rad. If the accuracy of beam energy measurement is required to be 1MeV, the uncertainty of the angle is $0.5\mu\text{rad}$ [5]. A small collision angle will reduce the interaction luminosity of Compton backscattering and the number of scattered photons. The repeatability and stability of the small collision angle are difficult to be controlled. (2) Replacing the CO_2 laser to a longer-wavelength light source. The light source required to generate the Compton scattered photon with the energy within 10MeV is the centimeter wave, also called a microwave.

In this paper, a new microwave-beam Compton backscattering method is proposed to measure the beam energy. In the head-to-head collision, it is possible to precisely measure the beam energy by detecting the maximum energy of the scattered photons. The scattered photons emit from the vacuum tube of the synchrotron radiation and the energy is detected by the HPGe detector. This method reduces the complexity of the system design and saves the cost. Considering the detection accuracy of the HPGe detector and reducing the influence of synchrotron radiation background, the maximum energy of the scattered photons is determined to be 9MeV. The energy of the initial photons is calculated to be $4.08 \times 10^{-5}\text{eV}$ by the Compton backscattering process. For $E = hc/\lambda$, the initial photons wavelength is 3.04cm, the frequency $f = c/\lambda$ is 10GHz. The measurement uncertainty of the beam energy can reach the order of 6MeV. In Sec. II, the principle of the interaction process and the system design of the entire beam measurement are introduced. In Sec. III, the number of scattered photons is obtained by calculating Compton backscattering cross section and luminosity. In Sec. IV, the simulation process. The shielding materials with 400cm polyethylene and 0.2cm lead are added to minimize the background noise. The influence of the hole radius on the cavity field and the influence of the hole radius on the resonance frequency are simulated by the CST software. In Sec. V, the discussion on the systematic error of the beam energy measurement.

II. INTERACTION PROCESS

A. Compton backscattering.

In 1948, Feenberg and Primakoff proposed the kinematics formula of the Compton scattering process[7]. The conservation of four momentum can be written as

$$p + k_0 \rightarrow p' + k, \quad (1)$$

where $p=(\varepsilon_0, \vec{p})$, $k_0=(\omega_0, \vec{k}_0)$ is the four momentum of the initial electrons and photons respectively; $p'=(\varepsilon, \vec{p}')$, $k=(\omega, \vec{k})$ is the four momentum of scattered electrons and photons respectively. Figure 1 shows the Compton backscattering process. The electrons collide with the photons at the angle α , resulting in scattered photons and scattered electrons.

According to the definition of Mandelstam variable of two-body scattering:

$$\begin{aligned} s &= (p + k_0)^2 = (p' + k)^2 = m^2 + 2\varepsilon_0\omega_0(1 - \beta\cos\alpha), \\ t &= (p' - p)^2 = (k - k_0)^2 = -2\omega_0\omega(1 - \cos(\alpha - \theta)), \\ u &= (p - k)^2 = (k_0 - p')^2 = m^2 - 2\omega\varepsilon_0(1 - \beta\cos\theta), \end{aligned} \quad (2)$$

where β is the electron velocity. Substituting Eq.(2) into $s + t + u = 2m^2$ and appropriately simplifying, the energy

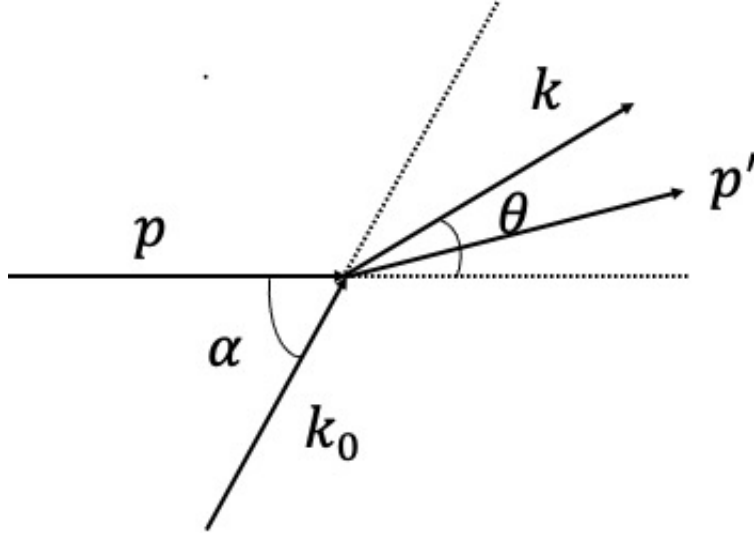


FIG. 1. The electrons and photons undergo Compton backscattering at the collision angle α , resulting in scattered photons and scattered electrons. α is the collision angle between initial electron and initial photon momenta. θ is the angle between initial electron and scattered photon momenta.

of the scattered photons is given by

$$\omega = \frac{\omega_0(1 - \beta \cos \alpha)}{1 - \beta \cos \theta + \frac{\omega_0}{\varepsilon_0}(1 - \cos(\alpha - \theta))}. \quad (3)$$

For $\theta = 0$, the maximum energy of the scattered photon is

$$\omega_{max} = \frac{\omega_0(1 - \beta \cos \alpha)}{1 - \beta + \frac{\omega_0}{\varepsilon_0}(1 - \cos \alpha)}. \quad (4)$$

For $\varepsilon_0 \gg m \gg \omega_0$, $\beta = \sqrt{1 - m^2/\varepsilon_0^2} \approx 1 - m^2/2\varepsilon_0^2$. Equation (4) can be simplified to be[8]

$$\omega_{max} = \frac{\varepsilon_0^2 \sin^2(\frac{\alpha}{2}) + \frac{m^2}{4} \cos \alpha}{\varepsilon_0 \sin^2(\frac{\alpha}{2}) + \frac{m^2}{4\omega_0}}. \quad (5)$$

If $\alpha = \pi$, then

$$\omega_{max} = \frac{\varepsilon_0^2 - \frac{m^2}{4}}{\varepsilon_0 + \frac{m^2}{4\omega_0}}. \quad (6)$$

Using Eq.(6), the beam energy can be written as follows:

$$\varepsilon_0 = \frac{\omega_{max}}{2} \left(1 + \sqrt{1 + \frac{m^2}{\omega_0 \omega_{max}}} \right). \quad (7)$$

The method of the microwave-beam Compton backscattering is applied to the Higgs mode of CEPC. Table 1 shows the parameters of the beam on CEPC[3]. The spectrum of scattered photons observed experimentally has a cutoff point at the maximum energy, known as the Compton edge. The maximum energy of scattered photons is obtained by fitting the Compton edge. Therefore, the beam energy is determined by Eq.(7). The number of scattered photons per second in Compton backscattering satisfies the following relationship

$$\frac{dN_\gamma}{dt} = L\sigma. \quad (8)$$

Equation.(8) are differentiated with energy ω ,

$$\frac{dN_\gamma}{d\omega dt} = L \frac{d\sigma}{d\omega}, \quad (9)$$

Parameters in the Higgs mode	Values
Beam energy ε_0 (GeV)	120
Bunch number B	242
Particles/bunch $N_2(10^{10})$	15
Bunch spacing (ns)	680
Beam current I (mA)	17.4
Bending radius ρ (km)	10.7
Beam size $\sigma_{x_2}/\sigma_{y_2}$ (μm)	200-450/5-20
Bunch length σ_{z_2} (mm)	4.4

TABLE I. CEPC parameters in Higgs mode. Taking the beam size $\sigma_{x_2} = 300\mu\text{m}, \sigma_{y_2} = 15\mu\text{m}$.

where the $\frac{d\sigma}{d\omega}$ is the interaction differential cross section. The number of scattered photons can be obtained after calculating the differential cross section and luminosity. The specific calculation process will be discussed in Sec. III.

B. Resonant cavity.

The incident photons are microwave photons with the resonance frequency of 10GeV. The transmission of microwave requires a guided wave system. The traveling wave propagates in the waveguide, and the standing wave is formed in the resonant cavity. The standing wave is stable, there is no movement of the energy in the direction of wave propagation. In the cylindrical cavity, there are three main resonant modes of TM_{mnp} , including TM_{010} , TE_{011} and TE_{111} . In TM_{010} , $m = 0, n = 1, p = 0$, the wave number $K = K_c = \frac{V_{01}}{R} = \frac{2.405}{R}$. The resonance frequency $f = K \cdot c/2\pi$ and resonance wavelength $\lambda = 2\pi/K = 2.613R$, where R is the radius of the cavity. Now the wavelength of the initial microwave photons is 3.04cm, the radius $R = 11.65\text{mm}$ for the cylindrical cavity can be determined. For the cavity length $l < 2.613R$, the TM_{010} is the main model of the cylindrical cavity. Figure 2 shows the resonant cavity and parameters. There are three coordinate systems, including the cylindrical coordinate system (r_1, φ_1, z_1) of the resonant cavity, the rectangular coordinate system (x_2, y_2, z_2) for the moving electron beam, the rectangular coordinate system (x, y, z) which is convenient for calculating. The electron beam passes through the side wall of the resonant cavity and undergoes Compton backscattering with microwave photons.

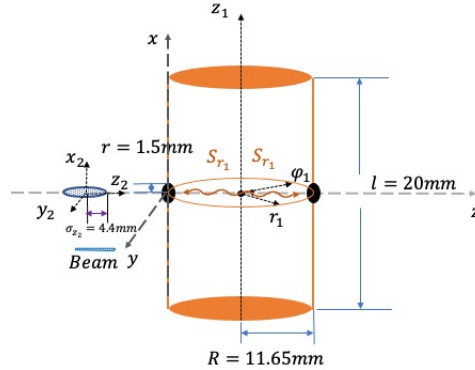


FIG. 2. The electron beam passes through the side wall of the resonant cavity and undergoes Compton backscattering with microwave photons. The S_{r_1} is the energy flux density of microwave photons. The direction of the microwave photons is in the radial direction of the cavity.

For the TM_{010} mode in the cylindrical coordinate system, the electromagnetic field is circularly symmetrical in the cavity[9]. The expression of the electromagnetic field in the resonant cavity is

$$E_{z_1} = E_m J_0(K_c r_1) e^{j\omega t}, \quad (10)$$

$$H_{\varphi_1} = jE_m \frac{1}{\eta} J_1(K_c r_1) e^{j\omega t}, \quad (11)$$

$$E_{r_1} = E_{\varphi_1} = H_{r_1} = H_{z_1} = 0, \quad (12)$$

where $\eta = \sqrt{\frac{\mu_0}{\varepsilon_0}}$, the vacuum permeability $\mu_0 = 4\pi \times 10^{-7} \text{H/m}$, the vacuum dielectric constant $\varepsilon_0 = 8.854188 \times 10^{-12} \text{F/m}$. It is known from Eq.(10), Eq.(11) and Eq.(12) that the electric field only has the longitudinal field in z_1 direction, the magnetic field only has the transverse field in the φ_1 direction. Figure 3 shows the electric field distribution in the transverse section and the magnetic field distribution in the longitudinal section of the resonant cavity. The electric field is in the z_1 direction, and the field strength weakens from the middle to the side walls. The magnetic field is in the φ_1 direction, and the field strength weakens from the sidewall of the cavity to the middle. The amplitude corresponds to 1J for energy stored in the cavity.

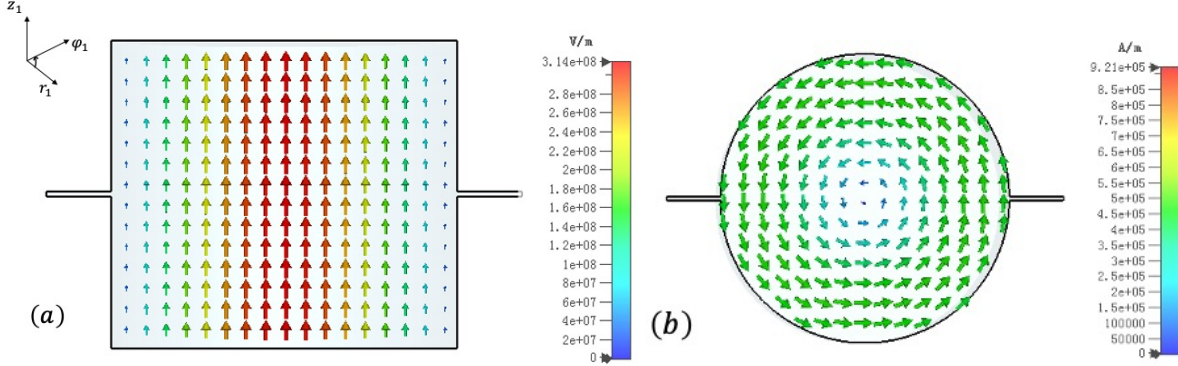


FIG. 3. The electric field distribution in the transverse section and the magnetic field distribution in the longitudinal section of the resonant cavity. (a) The electric field in the resonant cavity is in the z_1 direction, and the field strength weakens from the middle to the side walls. (b) The magnetic field is in the φ_1 direction, and the field strength weakens from the sidewall of the cavity to the middle.

The Poynting vector is the energy flow density vector in the electromagnetic field. According to the direction of the electromagnetic field, the Poynting vector is

$$\vec{S} = -\text{Re}(E_{z_1}) \times \text{Re}(H_{\varphi_1}) \vec{r}_1 = \frac{1}{\eta} E_m^2 J_0(K_c r_1) J_1(K_c r_1) \sin(\omega t) \cos(\omega t) \vec{r}_1, \quad (13)$$

where $\text{Re}(\cdot)$ means taking the real part. The Poynting vector $\vec{S} = S_{r_1} \vec{r}_1$. The S_{r_1} represents the energy per second passing through a vertical unit area. Figure 4 shows the distribution of Poynting vector \vec{S} , which is propagating from the central axis z_1 along the radius to the cavity wall. The field intensity of E_m is chosen to be equal to $1 \times 10^7 \text{V/m}$. The oscillation period $T = 5 \times 10^{-11} \text{s} = 50 \text{ps}$.

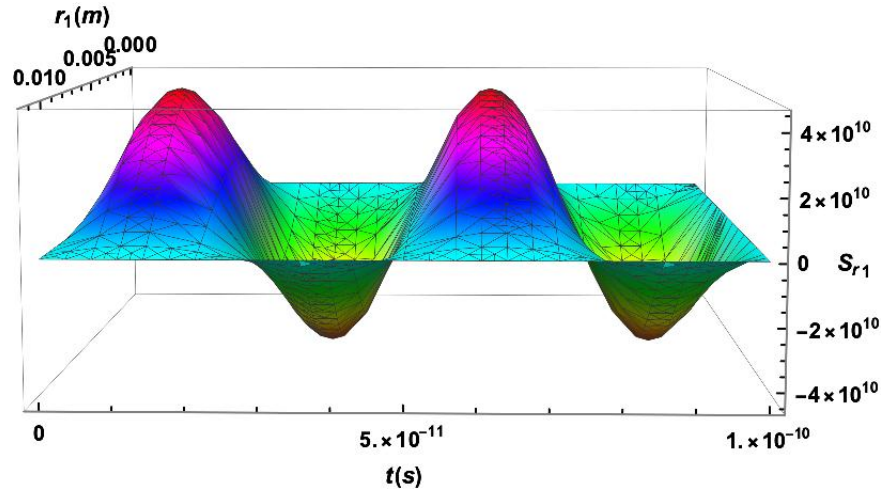


FIG. 4. The Poynting vector is propagating from the central axis z_1 along the radius to the cavity wall. The oscillation period $T = 50 \text{ps}$.

The direction of the microwave photons is the same as the \vec{S} . The $S_{r_1} < 0$ means the microwave photons are going in the opposite direction. As can be seen from Figure 2, the holes are made in the side wall of the cavity to let the electron beam pass through. Table 1 shows the bunch size $\sigma_{x_2} = 300\mu\text{m}$, $\sigma_{y_2} = 15\mu\text{m}$, $\sigma_{z_2} = 4.4\text{mm}$. The radius of the holes is adjustable within a certain range. It can be seen from Figure 11 that when the hole radius is 2mm, there is a 10% change between the local field of the hole and the field of the non-hole resonant cavity. If the hole radius is too small, the beam will hit the side wall of the cavity. The jitter up and down of the electron beam needs to be considered, and the radius of the hole is generally $3\sigma_{x_2}$ to $5\sigma_{x_2}$. The hole radius is $5\sigma_{x_2}$ about 1.5mm to allow the electron beam to pass through. In Sec. V will discuss the influence of the hole radius on the cavity field and the influence of the hole radius on the resonance frequency.

C. System design.

Figure 5 shows the design of the microwave-beam Compton backscattering system. The Compton backscattering occurs when the electron beam passes through the resonator cavity. The design is mainly divided into three parts, the first is the Compton backscattering process of microwave photons and electron beam; the second is the magnet separation system of scattered photons and scattered electrons, and the synchrotron radiation generated by the deflection of the electron beam under the magnetic field; the third is the detection system. The HPGe detector is used to detect the maximum energy of scattered photons. The shielding materials are designed to shield the low-energy synchrotron radiation photons.

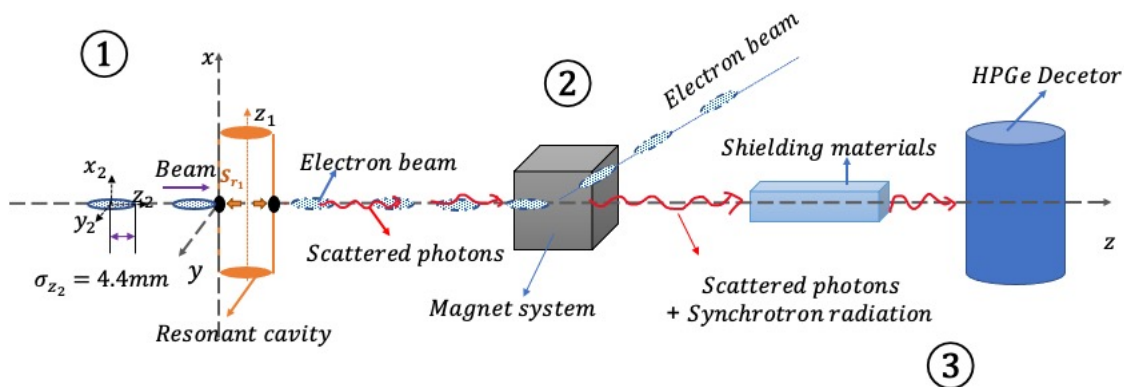


FIG. 5. The design of the microwave-beam Compton backscattering system. The design is mainly divided into three parts, the first is the Compton backscattering process of microwave photons and electron beam; the second is the magnet separation system of scattered photons and scattered electrons, and the synchrotron radiation generated by the deflection of the electron beam under the magnetic field; the third is the detection system. It is necessary to design shielding materials to shield the low-energy synchrotron radiation.

After Compton backscattering, the scattered photons and electrons are in the z direction. Figure 6 shows the separation system on CEPC between synchrotron radiation and electrons. The resonator cavity is placed before the separation system. Therefore, the microwave-beam method for beam energy measurement does not need to set up a new extraction system of scattering photons, which reduces the complexity of the system design and saves the cost. The scattered photons and the synchrotron radiation are output from the same channel, a shielding system is designed before the HPGe detector. The design of the shield, including materials and dimensions will be given in the Sec. IV.

III. CALCULATION PROCESS

A. Interaction cross section.

In a free space, the photons propagate in the form of plane electromagnetic waves. The cylindrical resonant cavity is bounded, the existence of boundary conditions creates a standing wave field in the cavity. The Compton backscattering

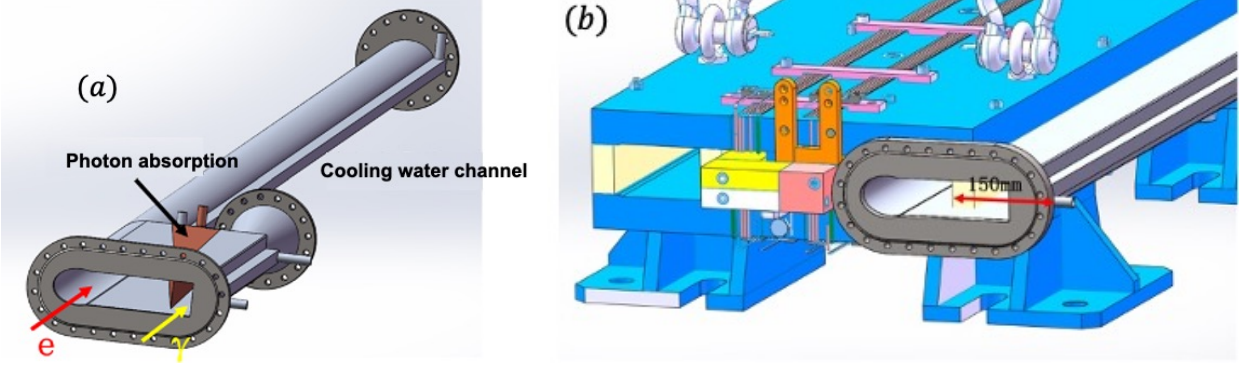


FIG. 6. The separation system on CEPC between synchrotron radiation photons and electrons. The (a) is a partial enlarged part of (b).

cross section in the resonant cavity is a little different from the cross section in a free space. In the reference [10], the cross section in the resonant cavity is equivalent to adding the coefficient $|F_{(TM010)}^{(1)}|^2$,

$$\frac{d\sigma_0}{d\omega} = |F_{(TM010)}^{(1)}|^2 \cdot 2\pi \frac{r_e^2}{\kappa^2(1+u)^3} \frac{\varepsilon_0}{(\varepsilon_0 - \omega)^2} \{ \kappa[1 + (1+u)^2] - 4\frac{u}{\kappa}(1+u)(\kappa - u) \}, \quad (14)$$

where $\kappa(\alpha) = 4 \frac{\omega_0 \varepsilon_0}{(mc^2)^2} \sin^2(\frac{\alpha}{2})$, the dimensionless constant $u = \frac{\omega}{\varepsilon_0 - \omega}$. The maximum energy of the scattered photons is 9MeV and the interaction angle $\alpha = \pi$, the energy of the initial microwave photons is $4.08032 \times 10^{-5} \text{eV}$. The differential cross section at 9MeV is about 0.04barn[10]. To get the number of scattered photons, it is necessary to calculate the interaction luminosity in the next step, which is related to the number of initial electrons and microwave photons.

B. Luminosity and the number of scattered photons.

The Poynting vector \vec{S} is divided by the energy of a single microwave photon ω_0 to get the areal density as follows

$$\vec{\sigma}_m = \frac{\vec{S}}{\omega_0} = \frac{1}{\eta\omega_0} E_m^2 J_0(K_c r_1) J_1(K_c r_1) \sin(\omega t) \cos(\omega t) \vec{r}_1', \quad (15)$$

where the unit is $1/(\text{m}^2 \cdot \text{s})$. The interaction luminosity of microwave photons and beam can be calculated by [11]

$$L = N_2 \cdot 2Bf' \int \sigma_m(r_1) f_2(x_2, y_2, z_2, t) dx_2 dy_2 dz_2 dt, \quad (16)$$

where N_2 is the number of electrons in a single bunch, B is the number of bunches, f' is the revolution frequency. For the single effect of a single electron bunch, $B = 1, f' = 1$. The normalization density function of one bunch, f_2 , can be written as

$$f_2(x_2, y_2, z_2, t) = \frac{1}{2\pi\sigma_{x_2}\sigma_{y_2} \cdot \sqrt{2\pi}\sigma_{z_2}} \exp \left[-\frac{1}{2} \left(\frac{x_2^2}{\sigma_{x_2}^2} + \frac{y_2^2}{\sigma_{y_2}^2} + \frac{z_2^2}{\sigma_{z_2}^2} \right) \right], \quad (17)$$

where $\int f_2(x_2, y_2, z_2, t) dx_2 dy_2 dz_2 = 1$. The parameters can be obtained from Table 1. The dimension of luminosity is $[1/\text{m}^2]$, which represents the number of particle collisions per unit area under a single electron bunch. The integration range is determined by the size of the electron bunch.

Figure 7 shows the schematic diagram of a single electron bunch passing through the resonant cavity. t_0 is defined as the moment when the beam reach the left wall of the cavity. The oscillation period of the microwave photons is 50ps. In the left part of z_1 , the beam and the microwave photons move in a head-to-head manner, and the beam will experience two complete wave packets. In the first wave packet, the overlapping length between the beam and the microwave photons is $5.626\text{mm}(c \cdot t_1)$; in the second wave packet, the overlapping length is an electron bunch

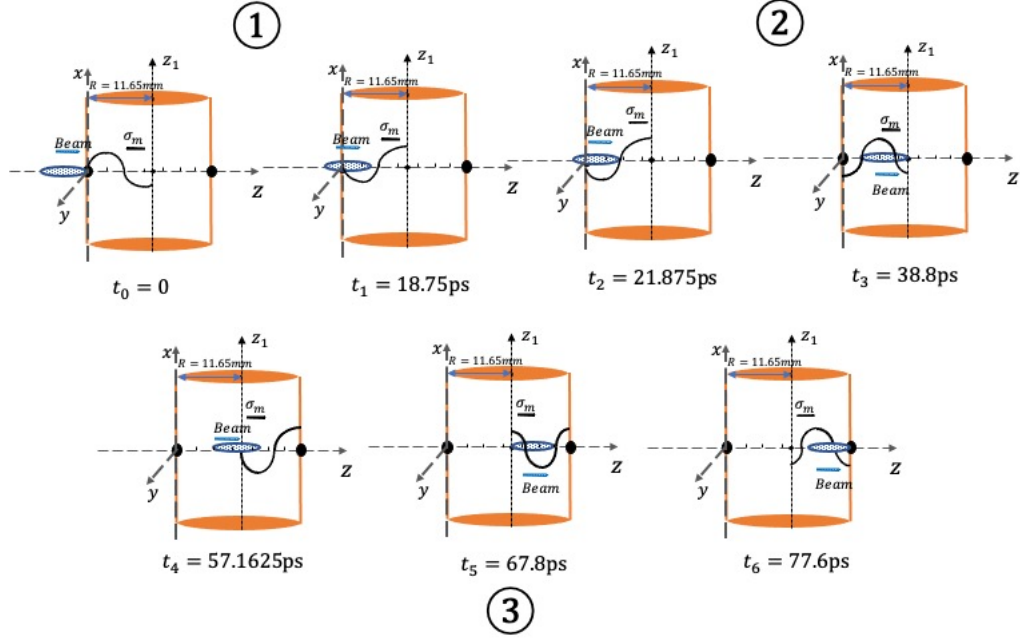


FIG. 7. The schematic diagram of a single electron bunch passing through the resonant cavity. The oscillation period of the microwave photons is 50ps. In the left part of z_1 , the beam and the microwave photons move in a head-to-head manner, and the beam will experience two complete wave packets. In the right part of z_1 , the beam and microwave photons move in the same direction at the speed of light c . For $\sigma_m < 0$, the head-to-head collision occurs.

length of 8.8mm from Table I. In the right part of z_1 , the beam and microwave photons move in the same direction at the speed of light c . For $\sigma_m < 0$, the head-to-head collision occurs. The overlapping length of the beam and the microwave photons is 5.509mm ($c \cdot (t_4 - t_3)$). Until it passes through the cavity from t_6 .

For $\omega_{max} = 9\text{MeV}$, the luminosity of the three parts is $4.30 \times 10^{33}/\text{m}^2$, $5.14 \times 10^{33}/\text{m}^2$, $3.18 \times 10^{33}/\text{m}^2$ respectively from Eq.(16). The differential cross section at 9MeV is $4 \times 10^{-30}\text{m}^2$ from Eq.(14). According to the Eq.(9), the number of scattered photons in the three parts is 17193, 20541, 12725 respectively. Therefore, an electron bunch passing through the resonant cavity will produce 50459 scattered photons. Another rough method is used to estimate the number of scattered photons from Compton backscattering. N_e is the number of beam electrons, N_{mp} is the number of microwave photons, σ is the cross-section of scattering. The number of scattered photons $N_\gamma = N_e \cdot N_{mp} \cdot \sigma/S$, where S is the cross-sectional area of interaction. As shown in Figure 7, the number of scattered photons is calculated in three parts. For example, in the first part, $N_{mp} = 1.4 \times 10^{15}$ and $N_e = 2.8 \times 10^{10}$ by integral, the $N_\gamma = 10945$. Therefore, the number of scattered photons that come out from three parts is 66896, which is no difference in order.

IV. SIMULATION PROCESS

A. Synchrotron radiation.

As the electron velocity approaches the speed of light, the angular distribution of electromagnetic radiation shrinks within a very narrow angular range in the direction of the electron's velocity. The radiation angle of a high-speed moving charged particle is estimated to be

$$\theta = \frac{1}{\gamma} \approx \frac{mc^2}{\varepsilon_0}. \quad (18)$$

For the 120GeV beam energy, the divergence angle is 0.0043mrad. The synchrotron radiation will travel more than a thousand meters to reach a range of 1cm, and the main intensity will still be distributed around an angle of 0. This will cause the synchrotron radiation photons and Compton scattered photons are difficult to distinguish in space. The synchrotron radiation spectrum is continuous, evenly distributed in the horizontal direction, with the strongest at the

center plane in the vertical direction. At the center plane of the light source radiation, the intensity is integrated in the vertical direction to obtain the photon flux F_{bm} as follows:

$$\frac{dF_{bm}(y)}{d\theta} = 2.457 \times 10^{13} E(\text{GeV}) I(A) G(y). \quad (19)$$

Taking one thousandth of the photon energy bandwidth, the unit of the photon flux is $photons/s/mrad/0.1\%BW$, θ is the horizontal observation angle. The I is the storage ring current, $I = 17.4\text{mA}$. The $G(y)$ is

$$G(y) = y \int_y^\infty K_{\frac{5}{3}}(y') dy, \quad (20)$$

where K is the second kind of modified Bessel function. $y = \epsilon/\epsilon_c$. ϵ is the photon energy. ϵ_c is the critical photon energy written as follows:

$$\epsilon_c = 2.218 \frac{E^3}{\rho}, \quad (21)$$

where the E is the energy of electrons, 120GeV in Higgs mode. From Table 1, The bending radius ρ is equal to 10.7km. The critical photon energy from Eq.(21) is 358.2keV. In Eq.(19), the single effect of a single bunch is considered, the horizontal observation angle is 0.2mrad. The flux spectrum of the synchrotron radiation is shown in Figure 8.

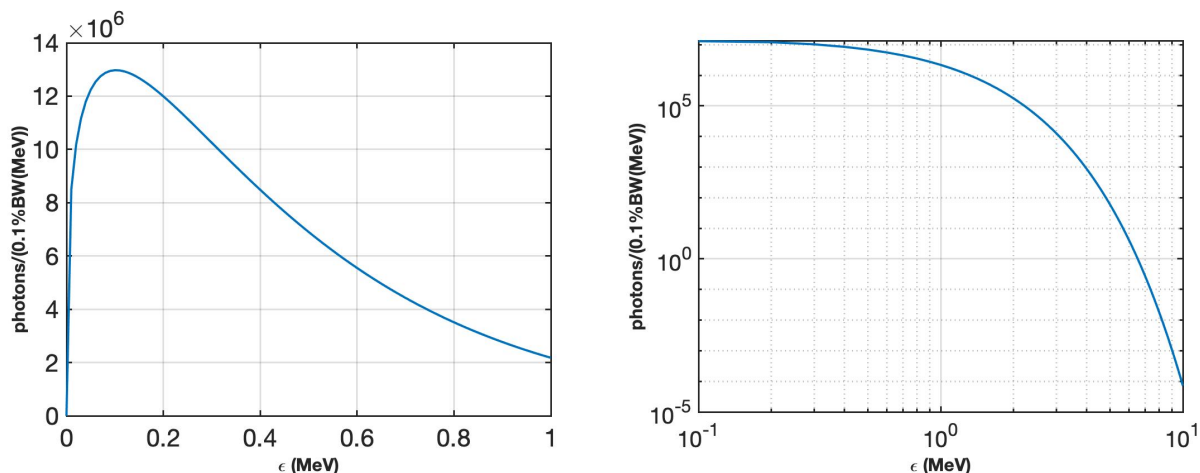


FIG. 8. The synchrotron radiation flux spectrum. (a) The energy range of photons is from 0 to 1MeV; (b) The energy range of photons is from 0 to 10MeV.

In order not to affect the detection of the scattered photons, the shielding materials should be designed to shield low-energy synchrotron radiation photons. In here, the number of 9MeV scattering photons and the synchrotron radiation photons flux spectrum were used as input sources, the shielding materials were added behind them. Recording the energy spectrum of the photons passing through the shielding materials to check if they can be distinguished. Figure 9 is the input sources for the Geant4 simulation. For the energy of scattering photons is 9MeV, the number of scattered photons is 50459 by Sec. *III – B*. The data of the synchrotron radiation flux spectrum is obtained from Figure 8. The synchrotron radiation photons are shielded by the polyethylene and lead target. It is concluded that the combination of 400cm polyethylene and 0.2cm lead have the best shielding effect on synchrotron radiation. Figure 10 shows the energy spectrum of photons after the lead target. It has reduce the number of low-energy synchrotron radiation photons. A P-type coaxial HPGc detector placed behind the lead target is used to detect the maximum energy of scattered photons. The diameter of the detector is 5-6 cm, and the height is about 5-7 cm. The detector is connected to multi-channel analyzer. Therefore, the maximum energy of scattered photons is obtained by fitting the Compton edge of the scattering photons energy spectrum[8].

B. Possible background

The energy storage and power loss of the cylindrical resonant cavity at the resonant frequency of 10GHz are calculated. The electromagnetic field is established, the field oscillation will be maintained. The energy will be

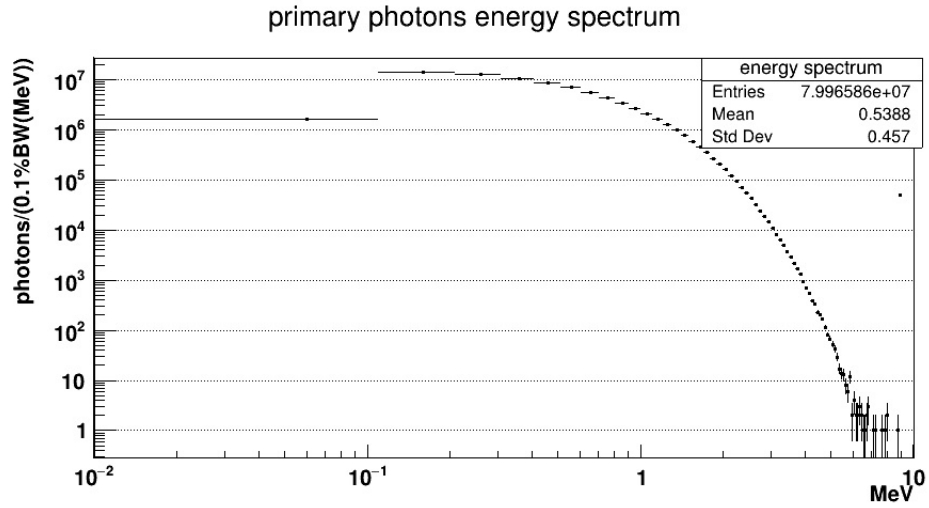


FIG. 9. The input sources for the Geant4 simulation. The number of scattered photons is 50459 when the energy is 9MeV by Sec. III – B. The data of the synchrotron radiation flux spectrum is obtained from Figure 9. The intensity of the two sources is 5.0459:7994.9541 with the total number is 8×10^7 .

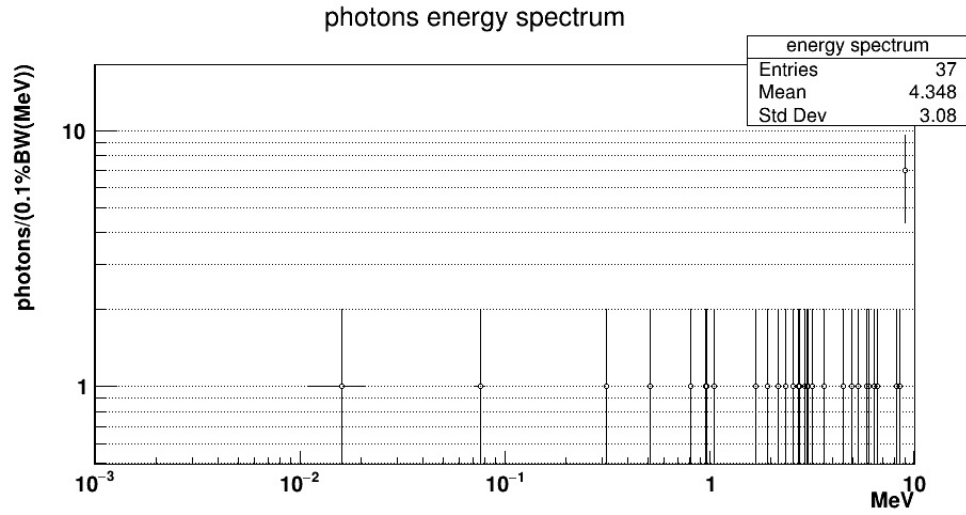


FIG. 10. The photons energy spectrum is obtained after passing through the shielding materials. The number of low-energy synchrotron radiation photons is reduced. It is easy to distinguish the scattered photons and the synchrotron radiation photons.

distributed throughout the space. At the resonance frequency, the maximum value of electric field energy storage is equal to the maximum value of magnetic field energy storage[12]. The energy storage in the cavity is

$$W = \frac{\varepsilon_0}{2} \cdot 2\pi l E_m^2 \int_0^R J_0^2\left(\frac{2.405}{R}r\right) r dr = \frac{1}{2} \pi \varepsilon_0 R^2 l E_m^2 J_1^2(2.4), \quad (22)$$

where the radius $R = 11.65\text{mm}$, the length of the cavity $l < 2.1R = 20\text{mm}$, $E_m = 1 \times 10^7\text{V/m}$. The energy storage can be calculated about 0.001J. The quality factor of the cylindrical resonant cavity is

$$Q = \frac{R}{\delta(1 + \frac{R}{l})}, \quad (23)$$

where the $\delta = \sqrt{\frac{2}{\omega\sigma\mu_0}}$ is the skin depth on the cavity wall. ω is the angular frequency. The conductivity $\sigma = 5.8 \times 10^7 \text{S/m}$.

The electromagnetic field has losses on the metal wall of the resonant cavity. The quality factor Q can be expressed as $\omega W/p_d$. According to the Eq.(22) and Eq.(23), the power loss p_d can be calculated about 6kw. The external excitation source can be fed with the same power, so that the loss and supplementation can reach a dynamic balance. At this time, the stored energy inside the resonant cavity is stable. The stability of the field is conducive to the Compton backscattering process. By the Eq.(23), the quality factor Q of the resonant cavity is obtained. Comparing the Q value from Eq.(23) with the results of the CST simulation including holes and without holes. Table II shows the parameters. Table III shows the variation of resonance frequency in the cavity with the hole radius 1mm, 1.5mm, and 2mm. The resonance frequency changes at a smaller extent with the radius increases. In order to ensure that the resonant frequency is consistent with the theoretical value, the size of the resonant cavity can be slightly adjusted.

parameter	frequency(GHz)	Q value
Theoretical calculation	9.848975	11055.4
Simulation (without hole)	9.848976	11048.2
Simulation (hole radius 0.15mm)	9.848973	11043.8

TABLE II. The resonance frequency and Q value of the cavity in theoretical calculation, simulation without holes and simulation with the 0.15mm hole radius.

hole radius/mm	frequency/GHz
1.0mm	9.84790
1.5mm	9.84533
2.0mm	9.84026

TABLE III. The variation of resonance frequency in the cavity with the hole radius 1mm, 1.5mm, and 2mm

The CST software is used to simulate the field strength in the cavity. Figure 11 shows the normalized distribution of the field. The theory and simulation almost overlap. The leakage field in the side wall is quickly cut off. After increasing the radius, the distribution of the field has only a slight change in the local part of the hole. The influence on the field can be ignored under the small hole radius. The influence on the resonance frequency can be corrected by fine-tuning the cavity size.

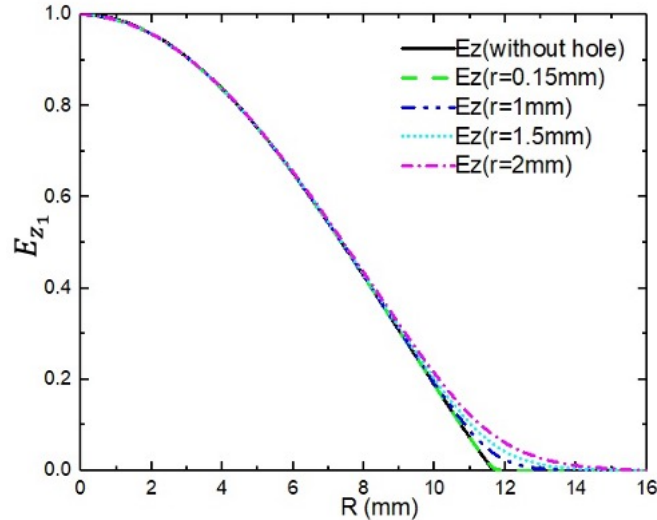


FIG. 11. The normalized distribution of the field in the direction of the cavity radius. The theory and simulation almost overlap. The leakage field in the side wall is quickly cut off. After increasing the radius, the distribution of the field has only a slight change in the local part of the hole. The influence on the field can be ignored under the small hole radius.

The electron bunches traverse the resonant cavity. Under the action of the strong electric field, the trajectory of electrons may shift. In the resonant cavity, the maximum field strength $E_m = 1 \times 10^7 \text{V/m}$, the average value

$\bar{E}_{z_1} = 6.11351 \times 10^6 \text{V/m}$ can be calculated by

$$E_{z_1} = E_m J_0(K_c r_1), \quad (24)$$

$$\bar{E}_{z_1} = \frac{\int_{-R}^R E_{z_1} dr_1}{2R}. \quad (25)$$

The energy in the theory of relativity is given by

$$E = \gamma m_0 c^2 = 120 \text{GeV}. \quad (26)$$

The influence can be estimated as follows:

$$F = q \bar{E}_{z_1} = \frac{\gamma m_0 c^2}{r}. \quad (27)$$

The deflection radius $r = 19.629 \text{km}$, the characteristic energy from Eq.(21) is 195.257keV . The influence of the magnetic field in the cavity can be calculated, and the deflection radius $r = 28.837 \text{km}$. The electromagnetic field radiation in the resonant cavity is smaller than the synchrotron radiation.

V. DISCUSS

A. Error Analysis.

The energy measurement uncertainty of the circular electron positron collider beam is required to be less than 10MeV . The cavity is placed perpendicular in the beam tube, the Poynting vector exists in the radius direction. The microwave photons collide with the electrons head-to-head, $\alpha \approx 180^\circ$. The collision angle α is determined by the installation of the initial microwave system. The process of the vertical installation can be calibrated by laser. The laser positioning accuracy is up to $5 \times 10^{-7} \text{rad}$ [13]. The stability of the high-frequency microwave source can reach $10^{-5} \sim 10^{-6}$. For $\omega_{max} = 9 \text{MeV}$, $\omega_0 = 4.08032 \times 10^{-5} \text{eV}$, the $\delta\omega_0 \approx 4.08 \times 10^{-10} \text{eV} \sim 4.08 \times 10^{-11} \text{eV}$. Therefore, the main part of the beam energy measurement uncertainty is the detection uncertainty of the maximum energy of scattered photons. The maximum energy of scattered photons is 9MeV . If the HPGe detector is calibrated well enough to achieve the detection accuracy of 10^{-4} . The beam energy measurement uncertainty $\delta\varepsilon_0$ is 6MeV by Eq.(7). The relative error $\delta\varepsilon_0/\varepsilon_0 = 5 \times 10^{-5}$. However, if the detection accuracy of the HPGe detector is 10^{-3} , the uncertainty $\delta\varepsilon_0$ of the beam energy measurement is 60MeV . The relative error $\delta\varepsilon_0/\varepsilon_0 = 5 \times 10^{-4}$. The measurement error of the maximum energy of the scattered photons is dominant, it is important to study the calibration method of the HPGe detector.

B. Experimental design.

The microwave-beam Compton backscattering is a new method to measure the beam energy. The parameters in this paper are from CEPC, and currently there is no such high energy electron beam for experimental verification. Therefore, we designed a simple experiment. The electron beam generated by the photocathode electron gun. The parameters are shown in Table IV.

Parameters	Value
Beam energy (MeV)	4-5
Bunch number	2
Charge/bunch (nC)	>2
Repeat frequency (Hz)	50

TABLE IV. The parameters of photocathode electron gun.

The reaction process remains unchanged. The process of Compton backscattering occurs between 5MeV electrons and microwave photons with energy $\omega_0 = 4.08 \times 10^{-5} \text{eV}$. From Eq.(6), it can be calculated that the energy of the scattered photons is 0.0155432eV , the wavelength is $79.8 \mu\text{m}$. It belongs to far-infrared light. The charge of a single bunch is greater than 2nC . Assuming it is 5nC , the number of electrons in a single bunch is 3×10^{10} . The size of the

bunch is taken as $\sigma_x = \sigma_y = 10\mu\text{m}$, $\sigma_z = 3\text{mm}$. The luminosity was calculated by a similar method to Sec. III – B. The number of scattered photons is 5165. The scattered photons can be detected by a far-infrared spectrometer. Assuming that a 0.05 Tesla magnet is used to deflect 5MeV beam electrons, the critical energy of the synchrotron radiation photons can be calculated as follows

$$\epsilon(\text{keV}) = 0.665E^2(\text{GeV})B(T) = 8.31 \times 10^{-7}\text{keV} \quad (28)$$

The synchrotron radiation photons generated by the bending magnet does not affect the detection of the scattered photons.

VI. SUMMARY

The beam energy measurement uncertainty of microwave-beam Compton backscattering can reach the order of 6MeV. The scattered photons emit from the vacuum tube of synchrotron radiation. Considering the performance of the HPGe detector and the influence of the synchrotron radiation, the maximum energy of scattered photons is 9MeV. For $\omega_{max} = 9\text{MeV}$, the number of scattered photons is 50459. In order to detect the energy of scattered photons, the combination of 400cm polyethylene and 0.2cm lead can meet the requirements. The simulation of CST software shows that the influence on the field can be ignored under the small hole radius, and the cavity size can be fine-tuned to correct the changes of the resonant frequency. The radiation from the electron beam in the resonant cavity is smaller than the synchrotron radiation. In the next step, a calibration method for the HPGe detector will be designed so that its detection accuracy can reach 10^{-4} . In terms of the simulation, the next step is to simulate the energy deposition of scattered photons in the detector to obtain the Compton spectrum and find the Compton edge. The experiment of the microwave photons and the electrons from the photocathode electron gun will be used to achieve the Compton backscattering process.

VII. ACKNOWLEDGMENT

This work is supported in part by National Natural Science Foundation of China (11655003); Innovation Project of IHEP (542017IHEPZZBS11820, 542018IHEPZZBS12427); the CAS Center for Excellence in Particle Physics (CCEPP); IHEP Innovation Grant (Y4545170Y2); Chinese Academy of Science Focused Science Grant (QYZDY-SSW-SLH002); Chinese Academy of Science Special Grant for Large Scientific Projects (113111KYBS20170005); National 1000 Talents Program of China; the National Key Research and Development Program of China (No.2018YFA0404300).

VIII. DATA AVAILABILITY

The data that support the findings of this study are available from the corresponding author upon reasonable request.

-
- [1] G. Aad et al. (ATLAS), Phys. Lett. B 716, 1 (2012), arXiv:1207.7214 [hep-ex].
 - [2] S. Chatrchyan et al. (CMS), Phys. Lett. B 716, 30 (2012), arXiv:1207.7235 [hep-ex].
 - [3] M. Dong et al. (CEPC Study Group), (2018), arXiv:1811.10545 [hep-ex].
 - [4] D. B. G.-W. P. e. a. Arnaudon, L., Zeitschrift für Physik C Particles and Fields 66, 45 (1995).
 - [5] G. Tang, S. Chen, Y. Chen, Z. Duan, and C. Zhang, Review of Scientific Instruments 91, 033109 (2020).
 - [6] J. Zhang, X. Cai, X. Mo, C. Fu, G. Tang, M. Achasov, N. Muchnoi, I. Nikolaev, and F. Harris, Nuclear Physics B 939, 391 (2019).
 - [7] E. Feenberg and H. Primakoff, Phys Rev 73, 449 (1948).
 - [8] M. N. Achasov, C. D. Fu, X. Mo, N. Y. Muchnoi, Q. Qin, H. Qu, Y. Wang, and J. Xu, Accelerator center (2008).
 - [9] H. Tian and C. Tian, “ Analysis on the principle and application of microwave technology,” (2012) pp. 000(036):156–156.
 - [10] M.-Y. Si and Y.-S. Huang.
 - [11] T. Suzuki, “ General formulae of luminosity for various types of colliding beam machines,” (1976).
 - [12] K. Zhang, “ Microwave principle and technology,” (2006).
 - [13] F. Zhu, Y. Li, and J. Tan, Optical and Precision Engineering 28, 817 (2020).